VOL. 18, NO. 24, DECEMBER 2023 ISSN 1819-6608
ARPN Journal of Engineering and Applied Sciences

www.arpnjournals.com

REMOVAL OF TOXIC HEAVY METAL BY A COST-FREE AND ECO-FRIENDLY BPAC NANOADSORBENT

Khairiah Khairiah[1], Hajar Mawaddah[1], Jafri Haryadi[1], Ridwanto Ridwanto[1], Mohd Awang Kechik[2], Ahmad Fudholi[3] and Islamiani Safitri[4]
[1]Universitas Muslim Nusantara Al Washliyah, Jl. Garu II A, Medan Amplas, Kota Medan, Indonesia
[2]Superconductivity and Thin Films Laboratory, Department of Physics, Universiti Putra Malaysia, Serdang, Selangor, Malaysia
[3]Solar Energy Research Institute, Universiti Kebangsaan Malaysia, Bangi, Selangor, Malaysia
[4]Physics Education, Labuhanbatu University, RantauPrapat, Indonesia
E-Mail: khairiahlubis@umnaw.ac.id

ABSTRACT

Water is a very important human need. In Indonesia, particularly on a large scale, the provision of clean and hygienic water is still centered in metropolitan areas and is run by city drinking water organizations. Upon examination of water samples taken from one of the sources, it was discovered that Fe, Mn, Zn, and Pb heavy metal concentrations (1.475, 1.684, 19.635, and 0.294 mg/L) exceeded the requirements for clean water for hygienic and sanitary reasons. Comparing adsorption to other methods, it is generally the easier, more efficient, cost-effective, environmentally friendly, and simple to use way. Banana peel-activated carbon (BPAC), banana peel-activated carbon chitosan (BPACh), banana peel glutaraldehyde activated carbon (BPACGl), and banana peel-activated carbon EdTA (BPACEd) have all been used in the synthesis of BPAC nanoadsorbents both without and with additives. According to the results of the AAS analysis, BPACh nanoadsorbents had a greater adsorption percentage than pure BPAC and other materials with additions. BPACh's crystal size was found to range from 7.5 nm at low temperature to 28.5 nm at high temperature, according to structural characterization. Aggregation was detected by surface morphological characterization, and the BPACh material's maximum carbon purity was 88.15%. Contact time and solution pH have an impact on adsorption. At a contact duration of 30 minutes, a stirring speed of 200 rpm, and a solution pH of 6 with 76.97%, the best adsorption took place. Toxic heavy metals can be removed more effectively with BPACh nanoadsorbents.

Keywords: BPAC nanoadsorbent, heavy metal, remediation, polluted water, activated carbon.

Manuscript Received 25 October 2023; Revised 13 February 2024; Published 29 February 2024

1. INTRODUCTION

Human life depends absolutely on water. In Indonesia, the majority of the population still lives in urban areas, where the city drinking water utility is in charge of managing the provision of clean, wholesome water (Adusei *et al*., 2022; Gameli *et al*., 2022). According to Government Regulation Number 66 of 2014 concerning Environmental Health, water samples from one of the sources have heavy metal results such as Fe, Mn, Zn, and Pb (1.475; 1.684; 19.635 and 0.294) mg/L, exceeding the standard limits for clean water suitable for use for hygienic purposes sanitation. Additionally, the water is cloudy and smells (Jaafari *et al*., 2020; Zare *et al*., 2018).

Ion exchange techniques, reverse osmosis, membrane-based filtration for precipitation of complex forms, electrocoagulation, precipitation, and adsorption are a few of the current techniques developed for the removal of heavy metal complexes from the aquatic environment. When compared to a number of other approaches, adsorption is typically the one that is more straightforward, highly effective, inexpensive, cost-free, and simple to use (Massoudinejad *et al*., 2019; Safari *et al*., 2019). Clay, inorganic polymers, zeolite, and activated carbon are only a few examples of the several types of adsorbents that have been created for the physical-chemical adsorption of heavy metal ion complexes (K. Khairiah, Frida, Sebayang, Sinuhaji, & Humaidi, 2021; Petcharoen & Sirivat, 2012). Alginate, chitosan, and starch, among other natural biopolymer-based adsorbents obtained from different biological tissues, have all been studied (Drbohlavova *et al*., 2010; K. Khairiah *et al*., 2023; Vaidyanathan *et al*., 2017). The creation of nano-based adsorbents from biomass waste, such as banana peel activated carbon (BPAC), in combination with additional additives including chitosan, EDTA, and glutaraldehyde is particularly intriguing and has not been well investigated (K. Khairiah, Frida, Sebayang, Sinuhaji, Humaidi, *et al*., 2021; Olaoye *et al*., 2020; Safari *et al*., 2019; Zare *et al*., 2018).

Bacteria are utilized as markers of pollution of the aquatic environment in addition to harmful heavy metals. The permissible limit for bacterial contamination in aquatic environments is 0 CFU/100ml for E. coli microorganisms and 50 CFU/100ml Total Coliforn according to Government Regulation Number 66 of 2014 (Drbohlavova *et al*., 2010; Petcharoen & Sirivat, 2012; Siregar *et al*., 2021). The quality of the environment is also lowered by the presence of metal and bacterial pollutants in the aquatic environment. Chitin, which is found in the outer shells of insects, fungus, and crustaceans, is processed to create chitosan, a biopolymer (Hu *et al*., 2021; Tang *et al*., 2021; Yu *et al*., 2021). One of the many uses for chitosan is as an ion binder or adsorbent. Chitosan has a higher efficiency in adsorbing metal ions when it is in the form of nanoparticles because it has a particular surface, small size, and quantum size effect. Additionally, because it can enter bacterial cells directly, chitosan in the form of nanoparticles has a strong action in preventing bacterial growth (Liang *et al*., 2021; X. Liu *et al*., 2021; Y. Liu, Huo, *et al*., 2021; Y. Liu, Pang, *et al*., 2021; Zhu *et al*., 2021).

High-level disinfectant glutaraldehyde is used as an alternate disinfectant to sterilize (Ahmad & Danish, 2018; Akpomie & Conradie, 2020; Ali *et al*., 2016a, 2016b; Annadurai *et al*., 2018; Hu *et al*., 2020; Kobiraj *et al*., 2011; Negroiu *et al*., 2021). Alkaline, neutral, and acidic Aldehydes and polymer forms vary depending on pH. Consequently, glutaraldehyde's antimicrobial action is impacted. It is anticipated that the addition of glutaraldehyde, a cross-linked substance with strong enough cross-linking, will boost the material's capacity for adsorption (Ali, 2017; Ali *et al*., 2016b; Munagapati *et al*., 2018; Shukla *et al*., 2020; Singh *et al*., 2020; Singh, Kumar, *et al*., 2018; Singh, Parveen, *et al*., 2018). Although EDTA is a substance used in the treatment of heavy metal toxicity (Li *et al*., 2016a; Saleh Jafer & Hassan, 2019; Shakoor & Nasar, 2017).

2. EXPERIMENTAL PROCEDURE

2.1 Materials and Synthesis

Banana peel, NaOH, HCl, chitosan, and glutaraldehyde were among the substances employed in this study, which was produced by Merck from CV. Amor Chemical Indonesia. Another material is also equated. Using preparation methods, banana peels are dried to eliminate dirt and other impurities and to lower their water content. After being ground into a powder using a mortar and pestle, sieving, and blending, the banana peels are then placed through High Energy Milling (HEM) (Abdulfatai *et al*., 2013; Dawodu *et al*., 2021; Li *et al*., 2016b). The milling process was run for 24 hours with a 30-minute pause between each 90-minute cycle. For ten hours, banana peels are carbonized at a low temperature of 250°C. Using a 25% concentrated HCl solution; the carbonization products were chemically activated. The banana peel powder is mixed with NaOH solution for two hours before being baked at 80°C for four hours to create activated carbon. AAS, SEM/EDX, BET/BJH, and XRD were used to characterize the banana peel activated carbon (BPAC) after it had been mixed with chitosan, glutaraldehyde, and EDTA at a ratio of 1:1 each.

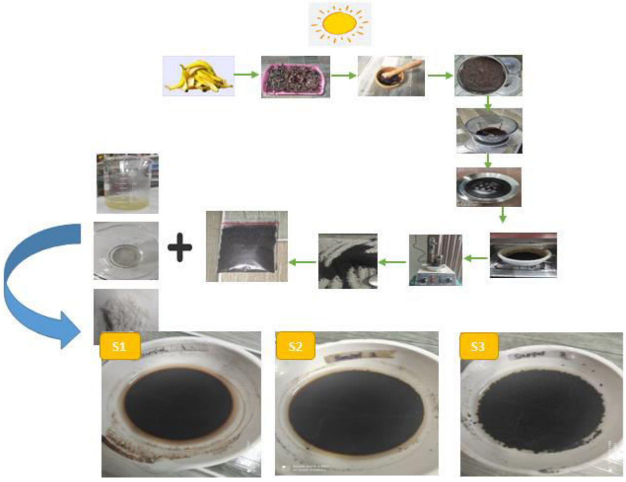

Figure-2.1. BPAC Synthesis.

2.2 Adsorption Study

The contaminated water was initially examined using AAS before conducting the adsorption investigation. Initial values of 1,475; 1,684; 19,635; and 0,294 mg/L for Mn, Fe, Pb, and Zn, respectively. According to these findings (Danish *et al*., 2018; Tejada-Tovar *et al*., 2018), the amount of numerous dangerous heavy metals in the water is higher than the allowable levels for good water quality. Variations in the experimental parameters, particularly temperature, stirring rate, and contact time, were used to examine the efficacy of heavy metals. The pH of the solution was adjusted to neutral (pH 7), and each adsorbent sample weighed 2 g (Abbas *et al*., 2014; El-sayed, 2020; Li *et al*., 2016c). The percentage of heavy metal removal can be calculated using the following formula:

$$\%Adsorption = \frac{C_o - C_e}{C_o} \times 100\%$$

With c_o : Initial Concentration (mg/l)
c_e : Final Concentration (mg/l)

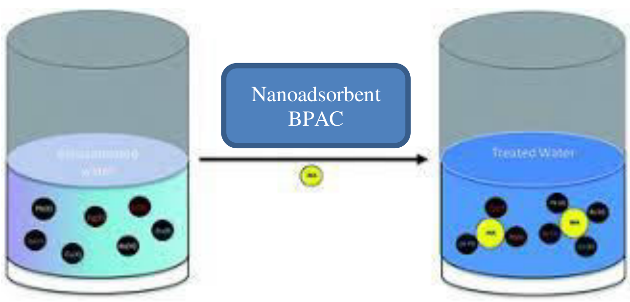

Figure-2.2. Adsorption process.

2.3 Adsorption Kinetics Modeling

Langmuir is one of the isothermic adsorption models. According to Langmuir, the amount of active sites on the surface of the adsorbent is proportional to its surface area (Lv *et al*., 2020; Mohamed *et al*., 2017; Mustapha *et al*., 2020). Physical or chemical bonds may form between the adsorbed material and the adsorbent.

VOL. 18, NO. 24, DECEMBER 2023 ISSN 1819-6608
ARPN Journal of Engineering and Applied Sciences

The following equation represents the linearization equation for the Langmuir isothermic adsorption model in a solution system.

$$\frac{c_e}{q_e} = \frac{1}{K_L q_{max}} + \frac{1}{q_{max}} c_e$$

With:

q_{max} : The maximum monolayer adsorption capacity of the adsorbent (mg/g)
K : Langmuir constant (L/mg)
c_e : Final Concentration (mg/l)

Pseudo-first-order and pseudo-second-order kinetic models can be used to study the kinetic model of heavy metal ion adsorption by the adsorbent in the solution system. (Lv *et al*., 2020; Marya *et al*., 2020; Okoli *et al*., 2018; Yuvaraja & Venkata, 2016). These models are advised for the same oleate, oxalate, and malonate adsorption on the adsorbent surface. As shown below, the equation (Wibowo *et al*., 2017):

$$\frac{dq_t}{d_t} = k_1(q_e - q_t)$$

Where q_e and q_t are the masses of adsorbate that are adsorbed on the surface of the adsorbent, and t is the adsorption contact time (Altun, 2019; Nithya & Sudha, 2016). Afterward, it is possible to formulate the initial first-order adsorption rate by

$$h_1 = k_1 q_e$$

The pseudo-second-order equation is as follows:

$$\frac{dq_t}{d_t} = k_2(q_e - q_t)^2$$

The pseudo-second-order initial adsorption rate is formulated as follows:

$$h_1 = k_1 {q_e}^2$$

2.4 Effect of Variations in Contact Time and pH

In the process of eliminating pollutants from polluted water, contact time is a crucial factor. Variations of 10, 20, 30, 40, and 50 minutes were used to study the evolution of contact time. Running it at 200 rpm allowed for the analysis of the stirring speed's results. By altering pH from 4, 5, 6, 7, and 8 while maintaining the same experimental settings, the impact of pH was examined.

2.5 Characterization

The Fe_3O_4 nanoadsorbent underwent adsorption tests on water contaminated with heavy metals. The BPAC nanoadsorbent is examined by utilizing an AAS (Atomic Absorption Spectroscopy) to identify the metal compounds in the water both before and after treatment. The best results were obtained by employing AAS, BET/BJH, SEM/EDX, and XRD to identify the functional groups produced on the BPAC nanoadsorbent. Metal compounds present in water that has not been treated and has been treated by BPAC nanoadsorbents are investigated by AAS characterisation. The parameters in 2.3 were used to calculate and assess the quality testing that was subjected to the BPAC nanoadsorbent in order to determine the efficiency value of the BPAC nanoadsorbent for the removal of heavy metals.

BET/BJH characterization was used to investigate the pore size and surface area of BPAC nanoadsorbents. The morphology and more precise composition of the BPAC nanoadsorbent are determined by SEM/EDS (Scanning Electron Microscope/Energy Dispersive X-Ray Spectroscopy). The phase formed from Fe_3O_4 nanoadsorbent powder was determined using XRD (X-Ray Diffraction). Calculation of crystal size with the Scherer

$$S = \frac{0{,}9\lambda}{B\cos\theta}$$

With

S = Crystal Size (nm)
λ = Wavelength (A).
B = FWHM (full width half maximum)(rad)
θ = Angle with High Intensity(^{o})

3. RESULTS AND DISCUSSIONS

3.1 % Adsorption

Variation in contact time has the goal of maximizing adsorption. The material in this instance contrasts BPAC, BPACh, BPACGl, and BPACEd. The BPAC nan adsorbent material was added to contaminated water as part of the adsorption process to determine its effectiveness in removing heavy metals. The contact period and acidity level allowed for the % adsorption results from the AAS characterization test to be seen. To ensure that the BPAC nanoadsorbent material is of the highest quality, this is done.

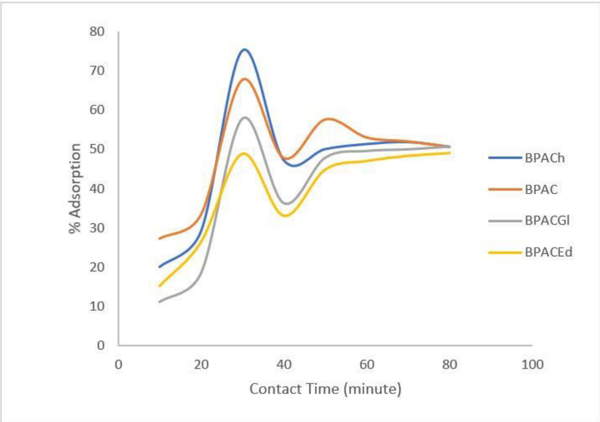

Figure-3.1. Effect of contact time variations.

ARPN Journal of Engineering and Applied Sciences

At this stage the adsorbent material used is BPAC nanocrystals without the addition of other materials, combined with chitosan, glutaraldehyde and EDTA which are added to polluted water to see how much effect they have on heavy metal removal. The % adsorption results obtained in the characterization test with AAS can be seen from the contact time in Figure-3.1. In Graph 3.1, it can be seen that the percentage adsorption of the four heavy metals (Mn, Fe, Pb, and Zn) reached 76.97% at a contact time of 30 minutes and a stirring speed of 200 rpm, then decreased again. This unique thing also happens to other materials. Compared to other studies reported, it is a striking finding, where the % adsorption was only 35.52% (Altun, 2019; Saikia *et al*., 2017; Wahyuningrum, 2014).

The pH of the solution is a significant parameter in % adsorption because it is related to the surface ionization of nanoparticles and heavy metal ions in polluted water. % adsorption was observed at pH 4, 5, 6, 7, and 8. It can be seen that the material with very high % adsorption is BPACh (banana peel activated carbon chitosan). Figure-3.2 shows that the highest % adsorption occurs at pH 6. The same thing happens with other materials.

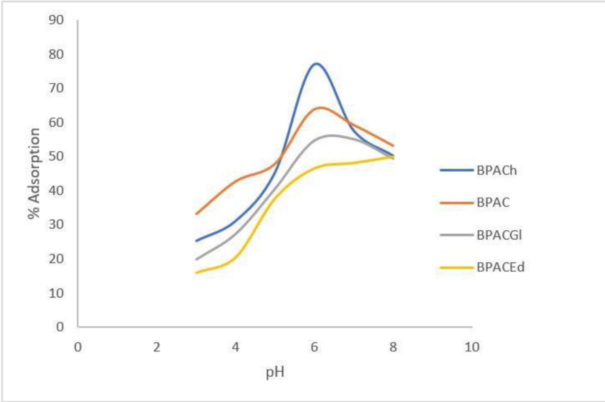

Figure-3.2. Effect of Variation of Solution pH.

It occurs in each material, whether it is BPAC, BPACh, BPACGl and BPACEd. However, the best performance is in BAPCh material for each heavy metal, as shown in Figure-3.2. The adsorption of various heavy metal ions (Mn, Fe, Pb, and Zn) was tested at the concentrations contained in polluted water, which had been successfully removed by % adsorption using BPAC material. It can be seen from the three graphs in Figures 3.1 and 3.2. These images show variations strongly influencing the % adsorption in pH and contact time. % Adsorption increased with increasing pH and contact time but decreased again when pH 6 was reached, the contact time was 30 minutes, and the stirring speed was 200 rpm. It occurs in all materials. It is because the active sites on the adsorbent become saturated under these conditions. From the observations, the characterization test of SEM/EDX, XRD and BET/BJH was the best material, namely BPAC with additional material chitosan with pH seven treatment, contact time of 30 minutes, and stirring speed of 200 rpm.

3.2 Adsorption Kinetics Modeling of Various Heavy Metals

The BET model analyzed the four heavy metal ions (Mn, Fe, Pb, and Zn). The graph can be seen in Figure-3.4, which shows a curved diagram. So this curvature proves the surface heterogeneity of the binding sites on BPAC nanoadsorbents. This model indicates that the BPAC nanoadsorbent is excellent and suitable for adsorbing the four heavy metals at different concentrations.

ISSN 1819-6608
ARPN Journal of Engineering and Applied Sciences

Table-1.1. Parameter of BET Isotermic.

Mn		Pb		Fe		Zn	
Ce (mg/L)	Ce/qe (g/L)	Ce (mg/L)	Ce/qe (g/L)	Ce (mg/L)	Ce/qe (g/L)	Ce (mg/L)	Ce/qe (g/L)
0,915	0,031017	0,0074	0,172568	0,185	0,074	0,0473	0,357928
0,713	0,02391	0,0102	0,115784	0,169	0,068699	0,11058	0,140713
0,577	0,019533	0,011107	0,10021	0,086	0,014862	0,076673	0,205547
0,491	0,017072	0,01564	0,061381	0,052	0,008228	0,10052	0,14813
0,609	0,028148	0,006516	0,179558	0,146	0,063368	0,022788	0,735914
0,897	0,085974	0,003067	0,410543	0,174	0,145	0,016067	1,053174
1,068	0,239309	0,001257	1,042841	0,195	0,413636	0,009177	1,864524

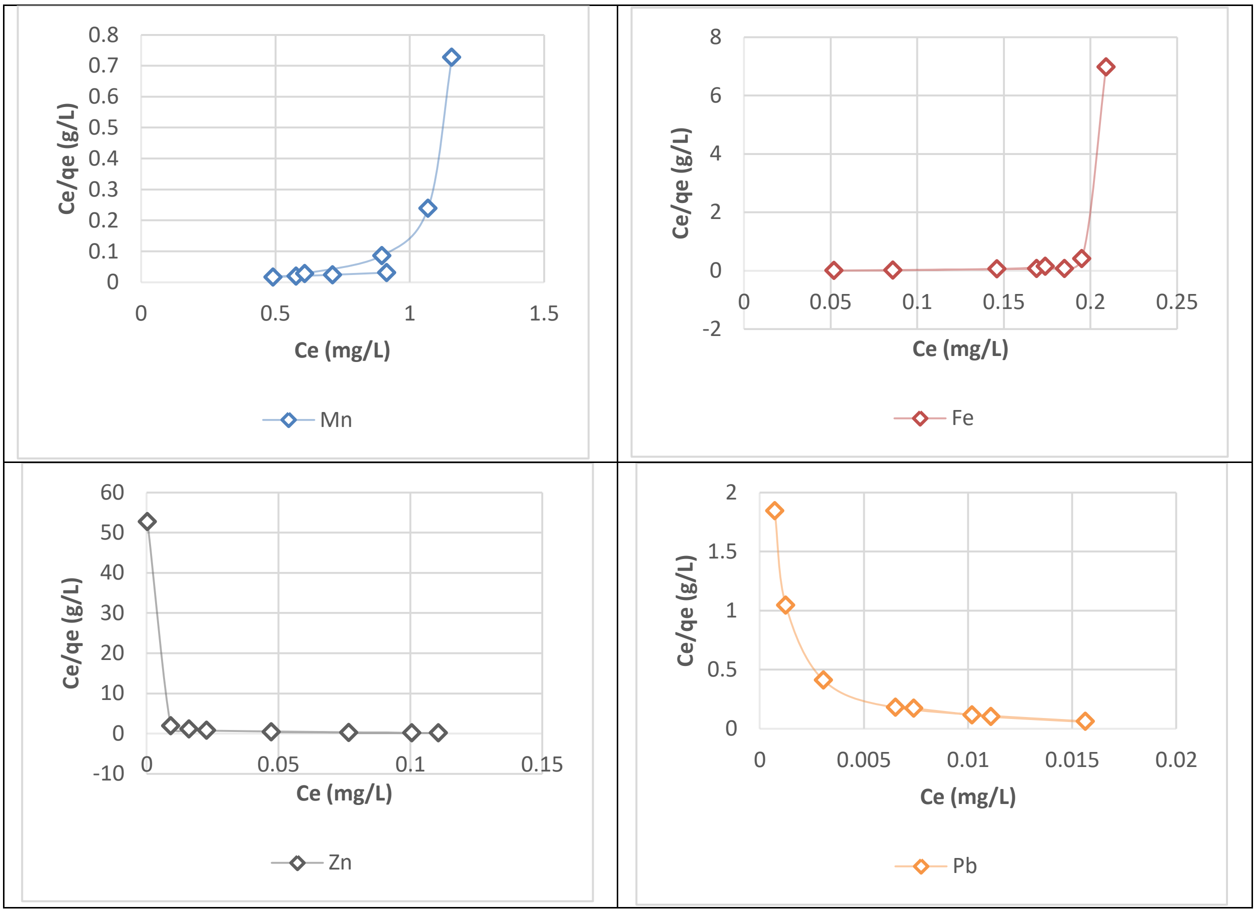

Figure-3.4. The BET Model.

The following adsorption kinetics analysis determines the adsorption reaction rate, adsorption constant, and adsorption rate based on calculations and plotted graphs as shown in Figure-3.5. The chart shows pseudo-first-order and pseudo-second-order. Pseudo-first-order shows sharp curvature in contrast to and pseudo-second-order. It happens because pseudo-second-order has high mobility compared to pseudo-first-order for all types of heavy metals. So it has a pseudo-second-order ability to interact with higher affinity sites.

ARPN Journal of Engineering and Applied Sciences

Table-3.1. Parameters of Adsorption Kinetics.

No	Initial Concentration (mg/l) C_o	Mean Q_e	Reaction Order	Reaction rate constant k	Absorption rate
1	Mn = 1.475	0,019468	Order 1	3,938983	0,076684
			Order 2	7,877966	1,20823
2	Fe = 1.684	0,006988	Order 1	4,963561	0,034685
			Order 2	9,927122	0,688652
3	Pb = 19.635	0,002634	Order 1	5,939252	0,015644
			Order 2	11,8785	0,371654
4	Zn = 0.294	0,047929	Order 1	3,038035	0,14561
			Order 2	6,076069	1,769472

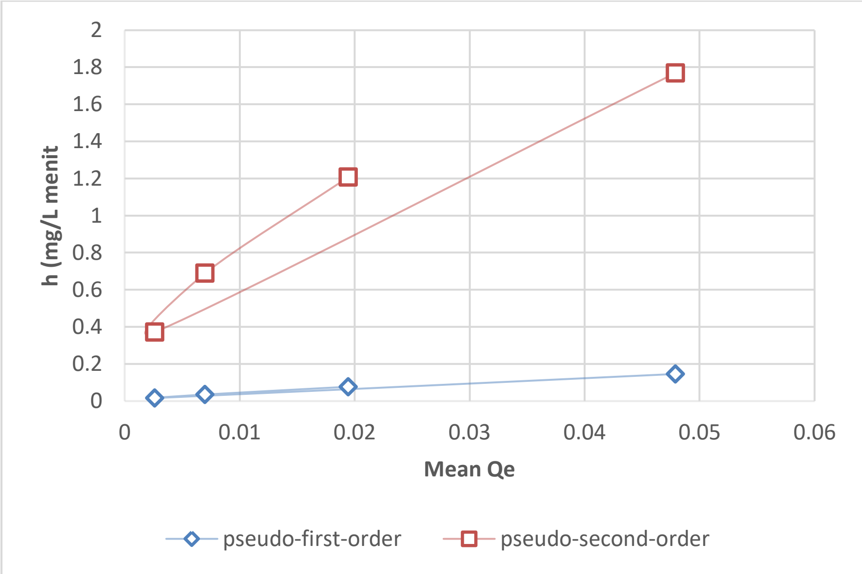

Figure-3.5. (a). Adsorption Kinetics Graph.

3.3 Interaction Mechanism

According to previous research, the mechanism of adsorption of heavy metal ions by adsorbed biomass adsorbed from a heterogeneous catalyst mechanism that takes place in a solution phase known as the Rideal-Eley-Langmuir-Hinshelwood mechanism which consists of five stages, namely.

- **Stage 1:** the process of diffusion or mass transfer of heavy metal ions from the bulk phase which has a higher concentration to the surface of the adsorbent which generally takes place quickly or sometimes takes place slowly.

- **Stage 2:** at this stage there is a process of chemisoption or physical absorption and heavy metal ions on the surface of the adsorbent, this stage generally takes place quickly.

- **Stage 3:** a chemical reaction or interaction occurs between heavy metal ions and active groups containing donor atoms of lone pair of atoms from the adsorbent component. This stage is generally slower than the other stages.

- **Step 4:** desorption of adsorbents of heavy metal ions bound to the active group of the adsorbent (if the type of adsorption is physical sorption). This stage is fast (Bondar *et al*., 2014; Giannakoudakis *et al*., 2018; J. H. Khairiah, 2020; K. Khairiah, Frida, Sebayang, Sinuhaji, & Humaidi, 2021; A. Liu *et al*., 2007).

The movement of heavy metal ion adsorbate molecules takes place randomly or randomly in the diffusion process. How far is the trajectory or distance traveled by the heavy metal ion adsorbate which moves randomly in the period t. It is assumed that the radius of the solvent is greater than the radius of the adsorbate of heavy metal ions. So among the four types of heavy metal ions, Mn ions are the easiest to experience the diffusion phenomenon in the adsorption mechanism of heavy metal ions by BPAC nanoadsorbent (Delaroza *et al*., 2020; Eny Kusriani, Diara D Kisnastiti, Lee D Wilson, Anwar

ARPN Journal of Engineering and Applied Sciences

Usman, 2018). Besides that, heavy metal ions which have smaller ionic radii have greater ionic mobility than heavy metal ions with larger ionic radius.

3.4 Characterization

The results of the analysis by XRD showed that BPACh (banana peel activated carbon chitosan) on the surface has a nearly 97% amorphous structure and a small portion of crystalline which is not visible on the diffractogram. This is consistent with the results of research which stated that in general natural biopolymer-based biomass has an amorphous structure in the 2α region between 17^o-22^o which is a typical area for amorphous materials containing activated carbon as shown in Figure-3.5.

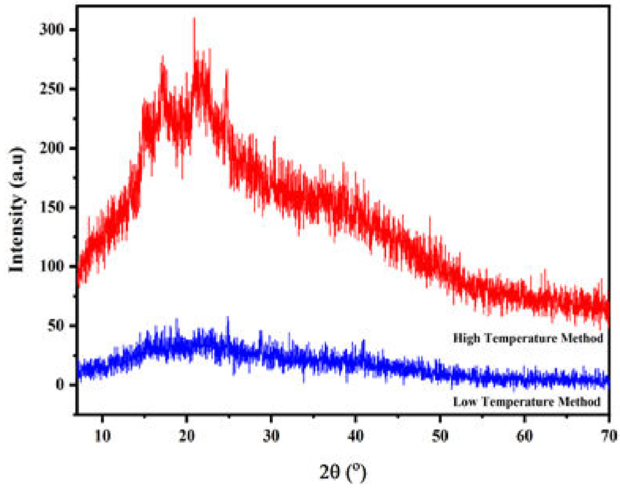

Figure-3.5. Diffraction pattern of BPACh.

Table-3.2. Data from XRD assistance from BPACh.

Sample	K	λ (Å)	Peak position 2θ (°)	FWHM B_{size} (°)	D (nm)	d(A)
BPACh	0,95	1,54178	32,5963	0,07930	7,55	2,74484
			28,8383	0,13670	10,34	3,09341
			28,6526	0,07870	7,88	3,11303
			29,5136	0,07130	9,49	3,03682
			38,3000	0,00000	10,89	2,34817
			49,5666	0,05330	8,43	1,83760
			58,0075	0,06500	9,14	1,58868

In Figure-3.5. It can be seen that there are 2 diffraction patterns from the XRD results of banana skin activated carbon, where for comparison/reference with different methods used, namely the high temperature method obtained in previous studies and in this study carried out with low temperature methods and modifications with HEM. The average size of the crystals obtained at low temperature is smaller than that at high temperature which is around 7.5 nm while at high temperature is around 28.5 nm.

SEM results on banana skin activated carbon with a modification method between low temperature carbonization and HEM (High Energy Milling) are shown in Figuress 3.6a, 3.6b, 3.6c and 3.6d

VOL. 18, NO. 24, DECEMBER 2023 ISSN 1819-6608
ARPN Journal of Engineering and Applied Sciences

www.arpnjournals.com

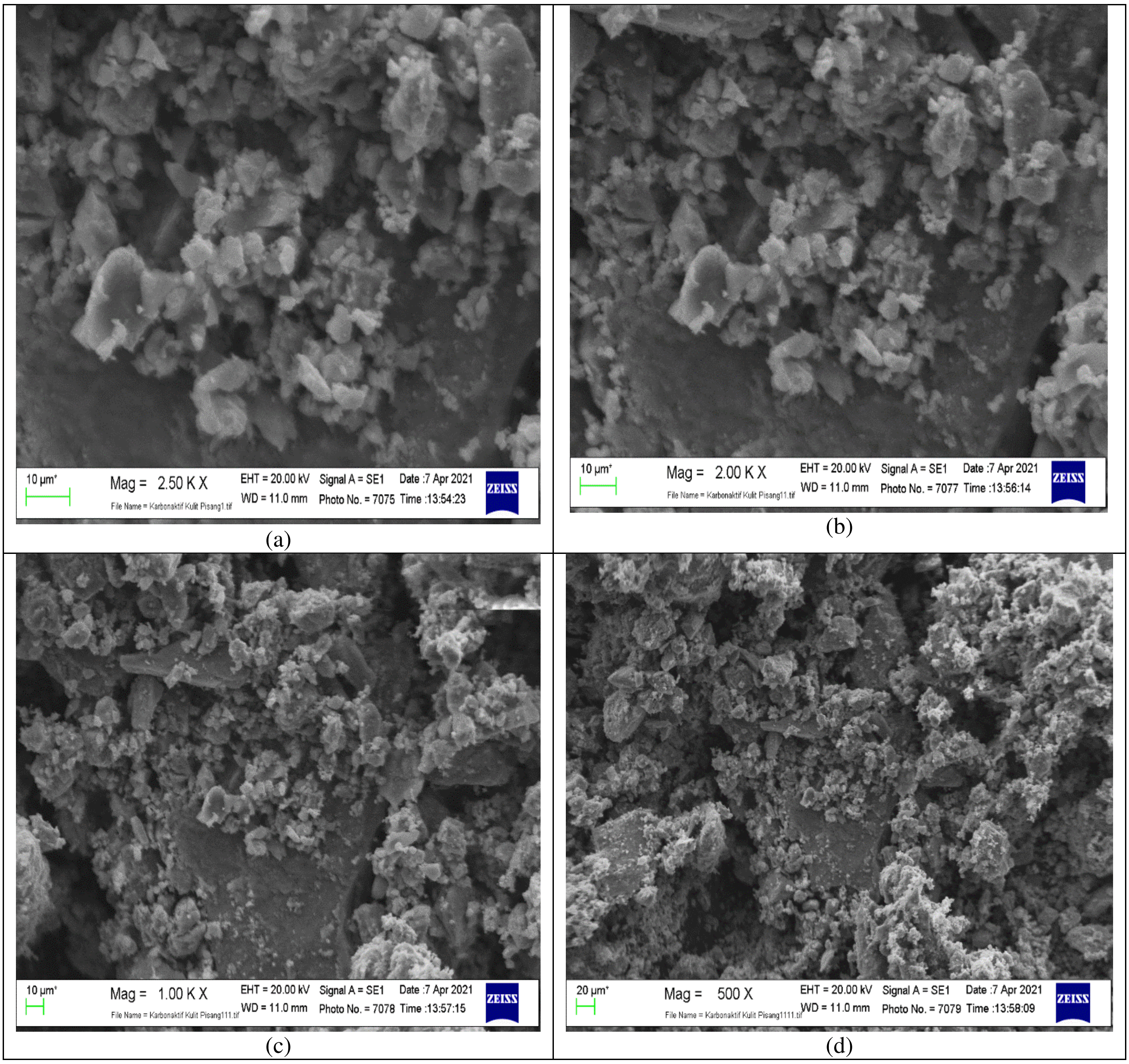

Figure-3.6. Surface morphology of BPACh Nanoadsorbent with various magnifications.
a. 2.5KX magnification. b. 2KX magnification. c. Magnification 1.0KX. d. 500X magnification

The SEM results, banana skin activated carbon is a porous material because there are cavities. The cavities formed are generated from a collection of aggregate particles that interact to form pores with a mesoporous scale (Eny Kusriani, Diara D Kisnastiti, Lee D Wilson, Anwar Usman, 2018; Kusumadewi *et al*., 2019). Other studies also reported that activated carbon from banana peel waste is a porous material. This supports and proves that banana peel activated carbon material can be doped with other materials, namely magnetic materials and chitosan in this study. To determine the mesoporous size of the banana skin activated carbon sample, a more accurate characterization was carried out using the BET/BJH method. The particle size is around 10 - 20µm, this size is quite large because the particles aggregate to form aggregates. While the analysis of the elemental content in the banana skin activated carbon sample used EDX which can be seen in Figure-3.7.

ISSN 1819-6608
ARPN Journal of Engineering and Applied Sciences

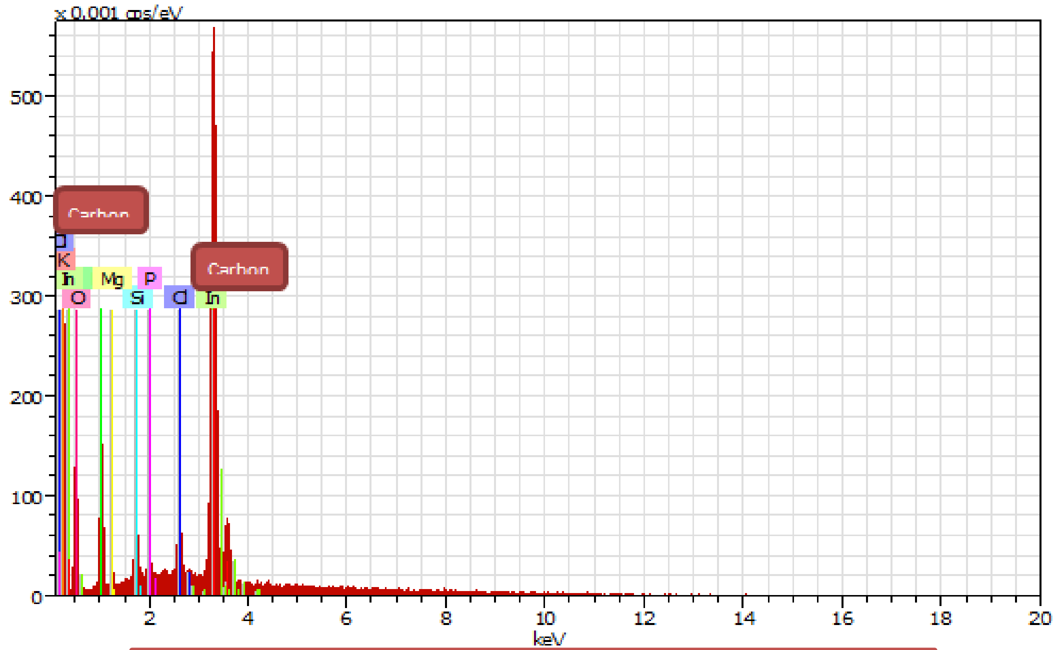

Spectrum : Banana Peel Activated Carbon Chitosan					
El AN corr.	Series	Unn. (wt %)	C norm. (wt %)	C Atom. (at %)	K. fact
C 6	**K-series**	**88,15**	**75,45**	**75,53**	**0,776**
O 8	K-series	10,52	3,15	3,85	0,207
K 19	K-series	1,25	1,92	1,87	0,006
Si 14	K-series	9,08	19,48	18,75	0,011
Total : 100.00					

Figure-3.7. Data from analysis of elemental content in activated carbon from banana peel waste with EDX.

The EDX analysis to determine the elemental content in banana skin activated carbon, it was found that element C was 88.15%, which can be seen in Figure-3.7. There are also other elements such as O, K, Si and others which are obtained from the synthesis of samples. These results indicate that the synthesis of activated carbon from banana peels with this modified method succeeded in obtaining a sufficiently maximum carbon value when compared to previous research, namely 63.24%.

a. BET/BJH

BET test results (Brunaeur Emmet Teller) and BJH (Barret Joyner Halenda) obtained the following results Figure-3.8: The BET Surface Area (specific area) is 159.85 m^2g. This value is relatively large which causes the weakness of banana peel activated carbon in absorbing heavy metal ions. This is because the banana peel activated carbon sample is only present on the surface of the water. BJH Adsorption desorption average pore diameter (average pore diameter of BJH adsorption and desorption) is 26.08 nm (Feng *et al*., 2021; Li *et al*., 2020; Thabede *et al*., 2021). As for the graph of the relationship between the relative pressure of nitrogen gas (P/Po) to the quantity adsorbed on the surface of the activated carbon of the banana peel (STP volume cc/g) it can be seen that starting at P/Po = 0.1 - 1.0 there is an increase in the adsorption of nitrogen gas which is very drastic and is known as the hysterical loop which describes the characteristics of the mesoporous diameter (Alamrani, 2021; Manyangadze *et al*., 2020). Where the mesoporous scale range from previous research is (2 - 50 nm).

ARPN Journal of Engineering and Applied Sciences

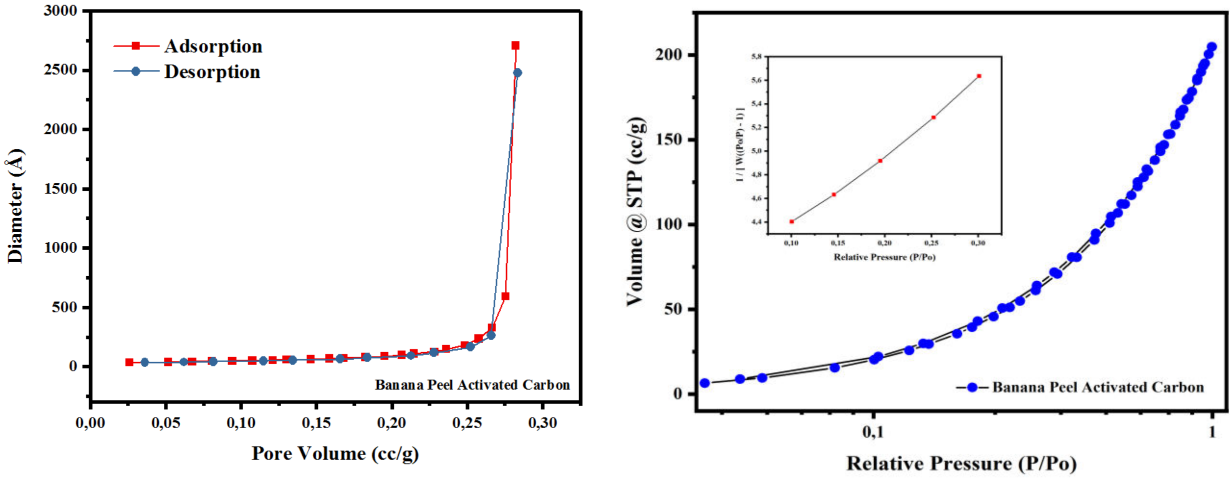

Figure-3.8. BET/BJH Graph.

4. CONCLUSIONS

In this study, the modification method, namely nanomaterials and carbonization, synthesized BPAC nanoadsorbents and remediated water contaminated with various heavy metals, namely Mn, Fe, Pb, and Zn. The experimental results show that % adsorption is affected by contact time and the pH of the solution. The optimum % adsorption occurred at a contact time of 30 minutes, a stirring speed of 200 rpm, and a solution pH of 6, which reached 76.97%. So from the four materials made it can be seen that the BPAC nanoadsorbent with the addition of chitosan called BPACh is more effective in remediating polluted water. This is supported by the results of SEM/EDX XRD and BET/BJH characterization.

ACKNOWLEDGMENT

Thanks to the Muslim Nusantara University Al Washliyah which has provided grants so that this research can be completed optimally.

REFERENCES

Abbas N. M., Firas S. A. and Suha I. A. 2014. Cyanide Removal From Wastewater by using Banana Peel. Journal of Asian Scientific Research. 4(5): 239-247.

Abdulfatai J., Saka A. A., Afolabi A. S. and Micheal O. 2013. Development of adsorbent from banana peel for wastewater treatment. Applied Mechanics and Materials, 248(December): 310-315. https://doi.org/10.4028/www.scientific.net/AMM.248.310

Adusei J. K., Agorku E. S., Voegborlo R. B., Ampong F. K., Danu B. Y. and Amarh F. A. 2022. Removal of Methyl red in aqueous systems using synthesized NaAlg-g-CHIT/nZVI adsorbent. Scientific African, 17, e01273. https://doi.org/10.1016/j.sciaf.2022.e01273

Ahmad T. and Danish M. 2018. Prospects of banana waste utilization in wastewater treatment: A review. Journal of Environmental Management, 206, 330-348. https://doi.org/10.1016/j.jenvman.2017.10.061

Akpomie K. G. and Conradie J. 2020. Banana peel as a biosorbent for the decontamination of water pollutants. A review. Environmental Chemistry Letters, 18(4): 1085-1112. https://doi.org/10.1007/s10311-020-00995-x

Alamrani N. A. 2021. Elimination of Congo Red Dye from Industrial Wastewater Using Teucrium polium L . as a Low-Cost Local Adsorbent. Adsorption Science & Technology, 2021.

Ali A. 2017. Removal of Mn(II) from water using chemically modified banana peels as efficient adsorbent. Environmental Nanotechnology, Monitoring and Management, 7(II): 57-63. https://doi.org/10.1016/j.enmm.2016.12.004

Ali A., Saeed K. and Mabood F. 2016a. Removal of chromium (VI) from aqueous medium using chemically modified banana peels as efficient low-cost adsorbent. Alexandria Engineering Journal, 55(3): 2933-2942. https://doi.org/10.1016/j.aej.2016.05.011

Ali A., Saeed K. and Mabood F. 2016b. Removal of chromium (VI) from aqueous medium using chemically modified banana peels as efficient low-cost adsorbent. Alexandria Engineering Journal, 55(3): 2933-2942. https://doi.org/10.1016/j.aej.2016.05.011

Altun T. 2019. Chitosan-coated sour cherry kernel shell beads: an adsorbent for removal of Cr (VI) from acidic solutions. Journal of Analytical Science and Technology. 6.

Annadurai G., Juang R. S. and Lee D. J. 2018. Adsorption of Heavy Metals from Water Using Banana and Orange Peels (PDF Download Available). Water Science and Technology. 185-190.

Bondar Y., Kuzenko S., Han D. and Cho H. 2014. Development of novel nanocomposite adsorbent based on potassium nickel hexacyanoferrate- loaded polypropylene fabric. 1-6.

Danish M., Ahmad T., Majeed S., Ahmad M., Ziyang L., Pin Z. and Shakeel Iqubal S. M. 2018. Use of banana trunk waste as activated carbon in scavenging methylene blue dye: Kinetic, thermodynamic, and isotherm studies. Bioresource Technology Reports, 3, 127-137. https://doi.org/10.1016/j.biteb.2018.07.007

Dawodu F. A., Abonyi C. J. and Akpomie K. G. 2021. Feldspar-banana peel composite adsorbent for efficient crude oil removal from solution. Applied Water Science, 11(1). https://doi.org/10.1007/s13201-020-01335-8

Delaroza R., Wijayanti A. and Kusumadewi R. A. 2020. The effect of mixing speed to adsorption heavy metal Cu 2 + and color using kepok banana peel waste. IOP Conference Series : Earth and Environmental Science. https://doi.org/10.1088/1755-1315/426/1/012024

Drbohlavova J., Hrdy R., Adam V., Kizek R., Schneeweiss O. and Hubalek J. 2010. Preparation and properties of various magnetic nanoparticles. Sensors, 9(4): 2352-2362. https://doi.org/10.3390/s90402352

El-sayed M. E. A. 2020. Nanoadsorbents for water and wastewater remediation. Science of the Total Environment, 739, 139903. https://doi.org/10.1016/j.scitotenv.2020.139903

Eny Kusriani, Diara D Kisnastiti, Lee D Wilson, Anwar Usman A. R. 2018. Adsorption Of Lanthanide Ions From An Aqueous Solution In Multicomponent Systems Using Activated Carbon From Banana Peels (Musa Paradisiaca L.). International Journal of Technology. 1132-1139.

Feng X., Sun S., Cheng G., Shi L., Yang X. and Zhang Y. 2021. Removal of Uranyl Ion from Wastewater by Magnetic Adsorption Material of Polyaniline Combined with CuFe 2 O 4. Adsorption Science & Technology. 2021.

Gameli B. H. R., Duwiejuah A. B. and Bawa A. A. 2022. Adsorption of toxic metals from greywater using low-cost spent green tea as a novel adsorbent. Scientific African, 17, e01296. https://doi.org/10.1016/j.sciaf.2022.e01296

Giannakoudakis D. A., Hosseini-bandegharaei A., Tsafrakidou P., Triantafyllidis K. S., Kornaros M. and Anastopoulos I. 2018. Aloe vera waste biomass-based adsorbents for the removal of aquatic pollutants: A review. Journal of Environmental Management, 227(September): 354-364. https://doi.org/10.1016/j.jenvman.2018.08.064

Hu B., Ai Y., Jin J., Hayat T., Alsaedi A., Zhuang L. and Wang X. 2020. Efficient elimination of organic and inorganic pollutants by biochar and biochar-based materials. Biochar, 2(1): 47-64. https://doi.org/10.1007/s42773-020-00044-4

Hu B., Wang H., Liu R. and Qiu M. 2021. Highly efficient U(VI) capture by amidoxime/carbon nitride composites: Evidence of EXAFS and modeling. Chemosphere, 274, 129743. https://doi.org/10.1016/j.chemosphere.2021.129743

Jaafari J., Barzanouni H., Mazloomi S., Amir Abadi Farahani N., Sharafi K., Soleimani P. and Haghighat G. A. 2020. Effective adsorptive removal of reactive dyes by magnetic chitosan nanoparticles: Kinetic, isothermal studies and response surface methodology. International Journal of Biological Macromolecules, 164, 344-355. https://doi.org/10.1016/j.ijbiomac.2020.07.042

Khairiah J. H. 2020. Potential Banana Husk Waste (Musa Paradisiaca) For An Adsorbent. International Journal of Scientific and Technology Research. 9(03): 1601-1604.
:

Khairiah K., Frida E., Sebayang K., Sinuhaji P. and Humaidi S. 2021. Data on Characterization, Model, and Adsorption Rate of Banana Peel Activated Carbon (Musa Acuminata) for Adsorbents of Various Heavy Metals (Mn, Pb, Zn, Fe). Data in Brief, 39, 107611. https://doi.org/10.1016/j.dib.2021.107611

Khairiah K., Frida E., Sebayang K., Sinuhaji P., Humaidi S. and Fudholi A. 2021. The Development of a Novel FM Nanoadsorbent for Heavy Metal Remediation in Polluted Water. South African Journal of Chemical Engineering, 39(July 2021): 32-41. https://doi.org/10.1016/j.sajce.2021.11.006

Khairiah K., Frida E., Sebayang K., Sinuhaji P., Humaidi S., Ridwanto, Fudholi A. and Marwoto P. 2023. Carboxymethyl Cellulose Nanoadsorbent for Remediation of Polluted Water. Journal of Ecological Engineering, 24(1): 336-348. https://doi.org/10.12911/22998993/156150

Kobiraj R., Nadeem U. and Chattopadhyaya M. C. 2011. Removal of copper from aqueous solution using eggshell as an adsorbent. Journal of the Indian Chemical Society. 88(6): 819-825.

Kusumadewi R. A., Wijayanti A. and Hadisoebroto R. 2019. Utilization of Banana Peel and Water Hyacinth Leaves as Adsorbent For Removal Of Copper From Wastewater. International Journal of Scientific & Technology Research. 8(12): 2529-2534.
.

Li Y., Liu J., Yuan Q., Tang H., Yu F. and Lv X. 2016a. A green adsorbent derived from banana peel for highly effective removal of heavy metal ions from water. RSC Advances, 6(51): 45041-45048. https://doi.org/10.1039/c6ra07460j

Li Y., Liu J., Yuan Q., Tang H., Yu F. and Lv X. 2016b. A green adsorbent derived from banana peel for highly effective removal of heavy metal ions from water. RSC Advances, 6(51): 45041-45048. https://doi.org/10.1039/c6ra07460j

Li Y., Liu J., Yuan Q., Tang H., Yu F. and Lv X. 2016c. A green adsorbent derived from banana peel for highly effective removal of heavy metal ions from water. RSC Advances, 6(51): 45041-45048. https://doi.org/10.1039/c6ra07460j

Li Y., Zimmerman A. R., He F., Chen J., Han L., Chen H., Hu X. and Gao B. 2020. Solvent-free synthesis of magnetic biochar and activated carbon through ball-mill extrusion with Fe3O4 nanoparticles for enhancing adsorption of methylene blue. Science of the Total Environment, 722, 137972. https://doi.org/10.1016/j.scitotenv.2020.137972

Liang L., Xi F., Tan W., Meng X., Hu B. and Wang X. 2021. Review of organic and inorganic pollutants removal by biochar and biochar-based composites. Biochar, 3(3): 255-281. https://doi.org/10.1007/s42773-021-00101-6

Liu A., Sun K. and Li A. 2007. Preparation of chitosan /carbon nanotubes composites. 143-147.

Liu X., Pang H., Liu X., Li Q., Zhang N., Mao L., Qiu M., Hu B., Yang H. and Wang X. 2021. Orderly Porous Covalent Organic Frameworks-based Materials: Superior Adsorbents for Pollutants Removal from Aqueous Solutions. The Innovation, 2(1): 100076. https://doi.org/10.1016/j.xinn.2021.100076

Liu Y., Huo Y., Wang X., Yu S., Ai Y., Chen Z., Zhang P., Chen L., Song G., Alharbi N. S., Rabah S. O. and Wang X. 2021. Impact of metal ions and organic ligands on uranium removal properties by zeolitic imidazolate framework materials. Journal of Cleaner Production, 278, 123216. https://doi.org/10.1016/j.jclepro.2020.123216

Liu Y., Pang H., Wang X., Yu S., Chen Z., Zhang P., Chen L., Song G., Saleh Alharbi N., Omar Rabah S. and Wang X. 2021. Zeolitic imidazolate framework-based nanomaterials for the capture of heavy metal ions and radionuclides: A review. Chemical Engineering Journal, 406, 127139. https://doi.org/10.1016/j.cej.2020.127139

Lv S., Li C., Mi J. and Meng H. 2020. Applied Surface Science a functional activated carbon for efficient adsorption of phenol derived from pyrolysis of rice husk, KOH-activation and EDTA-4Na-modi fi cation. Applied Surface Science, 510(November 2019): 145425. https://doi.org/10.1016/j.apsusc.2020.145425

Manyangadze M., Chikuruwo N. H. M., Narsaiah T. B., Chakra C. S., Radhakumari M. and Danha G. 2020. Enhancing adsorption capacity of nano-adsorbents via surface modi fi cation : A review. South African Journal of Chemical Engineering, 31(September 2019): 25-32. https://doi.org/10.1016/j.sajce.2019.11.003

Marya E., Alfatah T. and Dani M. 2020. Synthesis and characterization of activated carbon from Bambusa vulgaris striata using two-step KOH activation. Integrative Medicine Research, 9(3): 6278-6286. https://doi.org/10.1016/j.jmrt.2020.03.041

Massoudinejad M., Rasoulzadeh H. and Ghaderpoori M. 2019. Magnetic chitosan nanocomposite: Fabrication, properties, and optimization for adsorptive removal of crystal violet from aqueous solutions. Carbohydrate Polymers, 206(November 2018): 844-853. https://doi.org/10.1016/j.carbpol.2018.11.048

Mohamed N., Othman R., Mubarak N. M. and Chan E. 2017. Agricultural biomass-derived magnetic adsorbents : Preparation and application for heavy metals removal. Journal of the Taiwan Institute of Chemical Engineers, 78, 168-177. https://doi.org/10.1016/j.jtice.2017.05.023

Munagapati V. S., Yarramuthi V., Kim Y., Lee K. M. and Kim D. S. 2018. Removal of anionic dyes (Reactive Black 5 and Congo Red) from aqueous solutions using Banana Peel Powder as an adsorbent. Ecotoxicology and Environmental Safety, 148(August 2017): 601-607. https://doi.org/10.1016/j.ecoenv.2017.10.075

Mustapha S., Tijani J. O., Ndamitso M. M., Abdulkareem S. A. and Shuaib D. T. 2020. The role of kaolin and kaolin / ZnO nanoadsorbents in adsorption studies for tannery wastewater treatment. Scientific Reports, 1-22. https://doi.org/10.1038/s41598-020-69808-z

Negroiu M., Ţurcanu A. A., Matei E., Râpă M., Covaliu C. I., Predescu A. M., Pantilimon C. M., Coman G. and Predescu, C. 2021. Novel Adsorbent Based on Banana Peel Waste for Removal of Heavy Metal Ions from Synthetic Solutions. Materials, 14(14): 3946. https://doi.org/10.3390/ma14143946

Nithya R. and Sudha P. N. 2016. Removal of heavy metals from tannery effluent using chitosan-g-poly (butyl acrylate)/ bentonite nanocomposite as an adsorbent. Textiles and Clothing Sustainability, 1-8. https://doi.org/10.1186/s40689-016-0018-1

Okoli B. J., Shilowa P. M. and Modise J. S. 2018. Removal of Pb 2 + from Water by Synthesized Tannin Resins from Invasive South African Trees. Water, 1-14. https://doi.org/10.3390/w10050648

Olaoye R. A., Afolayan O. D., Adeyemi K. A., Ajisope L. O. and Adekunle O. S. 2020. Adsorption of selected metals from cassava processing wastewater using cow-bone ash. Scientific African, 10, e00653. https://doi.org/10.1016/j.sciaf.2020.e00653

Petcharoen K. and Sirivat A. 2012. Synthesis and characterization of magnetite nanoparticles via the chemical co-precipitation method. Materials Science and Engineering B: Solid-State Materials for Advanced Technology, 177(5): 421-427. https://doi.org/10.1016/j.mseb.2012.01.003

Safari E., Rahemi N., Kahforoushan D. and Allahyari S. 2019. Copper adsorptive removal from aqueous solution by orange peel residue carbon nanoparticles synthesized by combustion method using response surface methodology. Journal of Environmental Chemical Engineering, 7(1): 102847. https://doi.org/10.1016/j.jece.2018.102847

Saikia P., Bharali R. K. and Baruah H. K. 2017. Kinetic and thermodynamic studies for fluoride removal using a novel bio-adsorbent from possotia (Vitex negundo) leaf. Journal of Analytical Science and Technology. https://doi.org/10.1186/s40543-017-0132-y

Saleh Jafer A. and Hassan A. A. 2019. Removal of oil content in oilfield produced water using chemically modified kiwi peels as efficient low-cost adsorbent. Journal of Physics: Conference Series, 1294(7). https://doi.org/10.1088/1742-6596/1294/7/072013

Shakoor S. and Nasar A. 2017. Adsorptive treatment of hazardous methylene blue dye from artificially contaminated water using cucumis sativus peel waste as a low-cost adsorbent. Groundwater for Sustainable Development, 5, 152-159. https://doi.org/10.1016/j.gsd.2017.06.005

Shukla S. K., Al Mushaiqri N. R. S., Al Subhi H. M., Yoo K. and Al Sadeq H. 2020. Low-cost activated carbon production from organic waste and its utilization for wastewater treatment. Applied Water Science, 10(2): 1-9. https://doi.org/10.1007/s13201-020-1145-z

Singh S., Kumar A. and Gupta H. 2020. Activated banana peel carbon: a potential adsorbent for Rhodamine B decontamination from aqueous system. Applied Water Science, 10(8): 1-8. https://doi.org/10.1007/s13201-020-01274-4

Singh S., Kumar A., Gupta H., Mouiya M., Bouazizi A., Abourriche A., Benhammou A., El Hafiane Y., Ouammou M., Abouliatim Y., Younssi S. A., Smith A., Hannache H., Andreas A., Natalia E., Giovanni G., Memon J. R., Memon S. Q., Bhanger M. I., … Thomre K. 2018. Banana Peel: A Green Solution for Metal Removal from Contaminated Waters. Cogent Engineering, 7(2): 1487-1496. https://doi.org/10.5338/kjea.2013.32.2.108

Singh S., Parveen N. and Gupta H. 2018. Adsorptive decontamination of rhodamine-B from water using banana peel powder: A biosorbent. Environmental Technology and Innovation, 12, 189-195. https://doi.org/10.1016/j.eti.2018.09.001

Siregar, J., Septiani, N. L. W., Abrori, S. A., Sebayang, K., Irzaman, Fahmi, M. Z., Humaidi, S., Sembiring, T., Sembiring, K. and Yuliarto B. 2021. Review-A Pollutant Gas Sensor Based On Fe3O4 Nanostructures: A Review. Journal of the Electrochemical Society, 168(2): 027510. https://doi.org/10.1149/1945-7111/abd928

Tang H., Wang J., Zhang S., Pang H., Wang X., Chen Z., Li M., Song G., Qiu M. and Yu S. 2021. Recent advances in nanoscale zero-valent iron-based materials: Characteristics, environmental remediation and challenges. Journal of Cleaner Production, 319(August): 128641. https://doi.org/10.1016/j.jclepro.2021.128641

Tejada-Tovar C., Gonzalez-Delgado A. and Villabona-Ortiz A. 2018. Comparison of banana peel biosorbents for the removal of Cr (VI) from water. Contemporary Engineering Sciences, 11(21): 1033-1041. https://doi.org/10.12988/ces.2018.8390

Thabede P. M., Shooto N. D., Xaba T. and Naidoo E. B. 2021. Magnetite Functionalized Nigella Sativa Seeds for the Uptake of Chromium (VI) and Lead (II) Ions from Synthetic Wastewater. Adsorption Science & Technology, 2021(Ii).

Vaidyanathan G., Sendhilnathan S. and Arulmurugan R. 2017. Structural and magnetic properties of Co1-xZnxFe2O4 nanoparticles by co-precipitation method. Journal of Magnetism and Magnetic Materials, 313(2): 293-299. https://doi.org/10.1016/j.jmmm.2007.01.010

Wahyuningrum, H. 2014. Peat Water Treatment using Chitosan-Silica Composite as an Adsorbent. 8(3).

Wibowo E., Rokhmat M. and Abdullah M. 2017. Reduction of seawater salinity by natural zeolite (Clinoptilolite): Adsorption isotherms, thermodynamics and kinetics. Desalination, 409, 146-156. https://doi.org/10.1016/j.desal.2017.01.026

Yu S., Pang, H., Huang S., Tang H., Wang S., Qiu M., Chen Z., Yang H., Song G., Fu D., Hu B. and Wang X. 2021. Recent advances in metal-organic framework membranes for water treatment: A review. Science of the Total Environment, 800, 149662. https://doi.org/10.1016/j.scitotenv.2021.149662

Yuvaraja G. and Venkata M. 2016. Removal of Pb (II) ions by using magnetic chitosan-4- ((pyridin-2-ylimino) methyl) benzaldehyde Schiff's base. International Journal of Biological Macromolecules, 93, 408-417. https://doi.org/10.1016/j.ijbiomac.2016.08.084

Zare E. N., Motahari A. and Sillanpää M. 2018. Nanoadsorbents based on conducting polymer nanocomposites with main focus on polyaniline and its derivatives for removal of heavy metal ions/dyes: A review. Environmental Research, 162(December 2017): 173-195. https://doi.org/10.1016/j.envres.2017.12.025

Zhu Y., He X., Xu J., Fu Z., Wu S., Ni J. and Hu B. 2021. Insight into efficient removal of Cr(VI) by magnetite immobilized with Lysinibacillus sp. JLT12: Mechanism and performance. Chemosphere, 262(Vi): 127901. https://doi.org/10.1016/j.chemosphere.2020.127901